Cellular Microbiology (2011) **13**(7), 1044–1058
doi:10.1111/j.1462-5822.2011.01601.x
First published online 30 May 2011

Identification of a *Brucella* spp. secreted effector specifically interacting with human small GTPase Rab2

Marie de Barsy,[1†] Alexandre Jamet,[1,2†] Didier Filopon,[1] Cécile Nicolas,[1] Géraldine Laloux,[1] Jean-François Rual,[3‡] Alexandre Muller,[4,5,6] Jean-Claude Twizere,[7] Bernard Nkengfac,[1] Jean Vandenhaute,[1] David E. Hill,[3] Suzana P. Salcedo,[4,5,6] Jean-Pierre Gorvel,[4,5,6] Jean-Jacques Letesson[1] and Xavier De Bolle[1*]

[1]*URBM, University of Namur (FUNDP), Belgium.*
[2]*INRA, UMR1319 Micalis and AgroParisTech, UMR Micalis, F-78350 Jouy-en-Josas, France.*
[3]*Center for Cancer Systems Biology (CCSB) and Department of Cancer Biology, Dana-Farber Cancer Institute, and Department of Genetics, Harvard Medical School, Boston, MA 02115, USA.*
[4]*Centre d'Immunologie de Marseille-Luminy, Aix Marseille Université, Faculté de Sciences de Luminy, Case 906, Marseille, 13288 Cedex 9, France.*
[5]*INSERM, U631, Marseille, 13288, France.*
[6]*CNRS, UMR6102, Marseille, 13288, France.*
[7]*Center for Cellular and Molecular Biology, Gembloux ABT and GIGA research center, University of Liège, Belgium.*

Summary

Bacteria of the *Brucella* genus are facultative intracellular class III pathogens. These bacteria are able to control the intracellular trafficking of their vacuole, presumably by the use of yet unknown translocated effectors. To identify such effectors, we used a high-throughput yeast two-hybrid screen to identify interactions between putative human phagosomal proteins and predicted *Brucella* spp. proteins. We identified a specific interaction between the human small GTPase Rab2 and a *Brucella* spp. protein named RicA. This interaction was confirmed by GST-pull-down with the GDP-bound form of Rab2. A TEM-β-lactamase-RicA fusion was translocated from *Brucella abortus* to RAW264.7 macrophages during infection. This translocation was not detectable in a strain deleted for the *virB* operon, coding for the type IV secretion system. However, RicA secretion in a bacteriological culture was still observed in a Δ*virB* mutant. In HeLa cells, a Δ*ricA* mutant recruits less GTP-locked myc-Rab2 on its *Brucella*-containing vacuoles, compared with the wild-type strain. We observed altered kinetics of intracellular trafficking and faster proliferation of the *B. abortus* Δ*ricA* mutant in HeLa cells, compared with the wild-type control. Altogether, the data reported here suggest RicA as the first reported effector with a proposed function for *B. abortus*.

Received 16 September, 2010; revised 4 March, 2011; accepted 25 March, 2011. *For correspondence. E-mail xavier.debolle@fundp.ac.be; Tel. (+32) 81 72 44 38; Fax (+32) 81 72 42 97.
[†]These authors contributed equally to this work.
[‡]Present address: Department of Cell Biology, Harvard Medical School, Boston, MA 02115, USA.

Introduction

Bacterial pathogens of the *Brucella* genus are responsible of a worldwide zoonosis called brucellosis (Moreno and Moriyon, 2006). *Brucella* spp. are able to infect a wide range of mammals, including cows, sheep, goats, pigs, marine mammals, as well as humans (Moreno and Moriyon, 2006). The main symptoms include abortion or sterility in infected animals and Malta fever in humans (Moreno and Moriyon, 2006).

Brucellae are able to invade, survive and replicate in both professional and non-professional phagocytic cells. In several cell types, such as HeLa epithelial cells (Pizarro-Cerda *et al*., 1998) and bone marrow-derived macrophages (Celli *et al*., 2003), *Brucella abortus* is contained in a phagosome-derived vacuole called the *Brucella*-containing vacuole (BCV) and is able to control its intracellular trafficking, and particularly to move from a LAMP1-positive compartment similar to a late endosomal/lysosomal compartment towards a replicative vacuole carrying endoplasmic reticulum (ER) markers, thus bypassing lysosomal degradation (Celli and Gorvel, 2004). An ER-like replicative niche is consistent with the observation of *B. abortus* proliferating in ER-like compartments in trophoblasts of an infected goat, a natural host (Anderson and Cheville, 1986).

Cellular host factors critical for *B. abortus* intracellular proliferation, such as Sar1 GTPase (Celli *et al*., 2005), inositol-requiring enzyme 1 (Qin *et al*., 2008) and the Rab2 GTPase/GAPDH complex (Fugier *et al*., 2009), have been identified. In spite of this growing knowledge of

essential host factors for *Brucella* spp. replication, little is known about *Brucella* spp. mechanisms and molecular determinants allowing invasion and persistence in eukaryotic cells. In particular the effectors translocated (i.e. transported from the bacterium to the host cell) to control its trafficking remain unknown, although the type IV secretion system (T4SS) called VirB is activated in macrophages after phagocytosis and is necessary for *Brucella* spp. trafficking to ER-like compartments (O'Callaghan *et al*., 1999; Comerci *et al*., 2001; Delrue *et al*., 2001; Celli *et al*., 2003). The T4SS is thought to translocate effectors like those translocated by the Dot/Icm of *Legionella pneumophila* (Ensminger and Isberg, 2009). Two *B. abortus* proteins named VceA and VceC have been reported to be translocated to infected cells by a VirB-dependent process (de Jong *et al*., 2008) but their molecular functions remain unknown. The construction of a *Brucella melitensis* ORFeome (Dricot *et al*., 2004) allowed the set-up of genome-wide analyses aiming at identifying putative effectors. Here we report an original approach, using high-throughput yeast two-hybrid (HT-Y2H) screen, which allowed the identification of a bacterial effector able to interact with Rab2, a small GTPase described as recruited to the BCVs (Fugier *et al*., 2009). This is the first *Brucella* effector with a proposed function.

Results

Identification of RicA–Rab2 interaction using HT-Y2H

Using Y2H, we generated an interactome map between predicted *B. melitensis* proteins and the human proteins predicted to be associated to phagosomes, according to a proteomic study performed on mouse macrophages (Garin *et al*., 2001). Phagosome maturation is a cellular process controlled by *Brucella* spp., probably through the action of translocated bacterial effectors. We tested each of the 221 selected human open reading frames (ORFs) (the complete list is available in Table S1) from the human ORFeome (Rual *et al*., 2004; Lamesch *et al*., 2007) against the 3091 predicted coding sequences of the *B. melitensis* ORFeome (Dricot *et al*., 2004). The interacting pairs were identified (Table S2) as indicated in the *Experimental procedures*, resulting in a set of 38 *Brucella*–human Y2H interactions. Each one was individually retested after mating of the yeast strains carrying DB-ORF and AD-ORF fusions to yield 21 confirmed *Brucella*–human Y2H interactions (Table S3).

Among the 21 *Brucella*–human interspecies interactions found, four interactions involved GTPases. Those GTPases act as molecular switches that cycle between an inactive GDP-bound state and an active GTP-bound state (Colicelli, 2004). One interaction involved the *B. melitensis* ORF BMEI0736 and the human small GTPase Rab2, a protein recently shown as essential for intracellular replication of *B. abortus* (Fugier *et al*., 2009). Moreover, Rab2 is essential for Golgi-to-ER vesicle trafficking (Seabra *et al*., 2002), a trafficking pathway important for the intracellular replication of *B. abortus* (Fugier *et al*., 2009). BMEI0736 ORF is not located near genes putatively encoding a known secretion system (data not shown). BMEI0736 encodes a 175 amino acid protein sharing a weak similarity with acetyltransferases of the gamma carbonic anhydrase-like family, we named this protein RicA (Rab2 interacting conserved protein A). RicA is conserved in many α-proteobacteria, and many other taxons, including Gram-positive bacteria such as *Clostridium botulinum* (*E* value 9.10^{-36}), and even Archea like *Pyrococcus furiosus* (*E* value 4.10^{-36}).

We tested whether RicA specifically interacts with Rab2 using a set of 103 individual preys, extracted from the hORFeome v1.1 (Rual *et al*., 2004), encoding GTPases homologous to small GTPases (Table S4). Using Y2H, we tested the interaction of 103 individual DB-GTPase fusions against the AD-RicA fusion and, as expected, we confirmed the interaction between Rab2 and RicA. However, no interaction was detectable with the 102 other proteins tested (data not shown), even with the small GTPase Rab14, which shares the highest percentage of identity with Rab2 (58%). Thus, RicA specifically interacts with Rab2. Two other *B. melitensis* ORFs interacted with 7 or 13 preys among the 103 GTPases homologues, suggesting that they are non-specific interactors in this assay.

RicA preferentially interacts with GDP-bound GST-Rab2

The binding of GDP or GTP induces conformational changes of small GTPases, allowing them to interact with specific partners in a nucleotide-dependent manner (Takai *et al*., 2001). Because RicA interacts with Rab2, we postulated that this recognition could be dependent on a particular nucleotide-bound state of the GTPase. To test this hypothesis, a 3Flag tagged version of RicA was tested in a pull-down experiment with a GST-Rab2 fusion previously loaded or not with GDP or GTPγS, a non-hydrolysable GTP analogue. We observed that 3Flag-RicA preferentially binds to the GDP-bound GST-Rab2 compared with the nucleotide-free GST-Rab2 while the interaction is almost lost when GST-Rab2 is incubated with GTPγS (Fig. 1). These results suggest that RicA is not a GAP (GTPase activating protein), as GAPs interact with GTP-bound forms of the GTPases, and could act on Rab2 as a GDI (GDP dissociation inhibitor) or a GEF (guanine nucleotide exchange factor), because these two types of factors interact with GDP-bound forms of the GTPases. GEF activity was assayed using mant-GDP, a fluorescent analogue of GDP (Hemsath and Ahmadian,

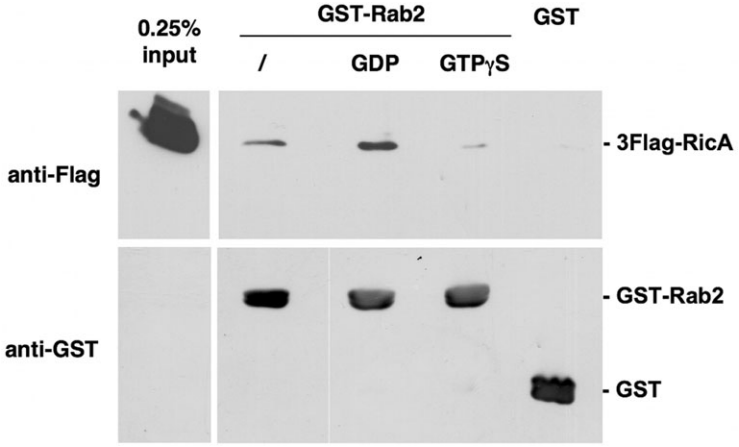

Fig. 1. 3Flag-RicA interacts with GST-Rab2. Upper part: Western blot using M2 anti-Flag antibody detecting 3Flag-RicA pulled-down from a bacterial lysate by GST-Rab2. 3Flag-RicA bacterial lysate (input) was used as a positive control for the 3Flag detection (0.25% of the quantity used in the pull-down was loaded). Lanes labelled with GDP or GTPγS indicate nucleotides added to the GST-Rab2 beads before pull-down. Beads loaded with GST alone were used as a negative control. Lower part: GST and GST-Rab2 fusions were detected with an anti-GST antibody.

2005). GST-Rab2 was purified and the kinetics of mant-GDP dissociation was followed to monitor the GDP/GTP exchange. As expected the mant-GDP binding to GST-Rab2 was relatively stable, and EDTA stimulated mant-GDP dissociation from GST-Rab2. However, purified His_6-RicA was not able to stimulate GDP/GTP exchange, even when equimolar concentrations of His_6-RicA and GST-Rab2 were used (data not shown). These data suggest that RicA is not a GEF for Rab2.

When HeLa cells are transfected with plasmids encoding HA-RicA and a myc-Rab2 form, either wild type, GDP-locked (N119I) or GTP-locked (Q65L), a cytosolic colocalization is observed with the GDP-locked form of myc-Rab2, but not with the two other forms of myc-Rab2 (Fig. 2). These data are consistent with a preferential interaction of RicA with the GDP-locked form of Rab2 in a cellular context.

RicA is translocated to host cells and secreted in bacterial cultures

In order to test translocation of RicA from the bacterium to the host cell, we used a TEM-β-lactamase-RicA fusion produced from a pBBR1-derived plasmid. As a positive control, we used the TEM-β-lactamase-VceA fusion, previously reported as translocated in a T4SS-dependent manner (de Jong *et al*., 2008). The TEM-β-lactamase alone was used as a negative control. The host cells

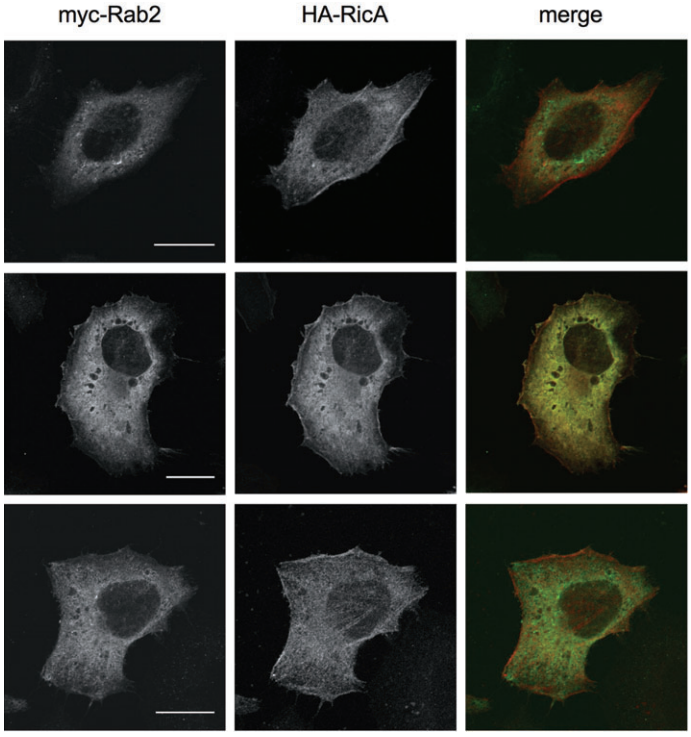

Fig. 2. Cytosolic localization of HA-tagged RicA is similar to the localization of a GDP-locked myc-Rab2(N119I) form. HA-RicA was produced after transfection with the pCMV-HA-ricA plasmid. A representative cell is shown for each form of myc-Rab2, as indicated on the right. In the left panels, immunofluorescence was made with an anti-myc antibody, in the middle panels immunofluorescence was made with the anti-HA antibody, and the right panels were generated by merging the anti-myc and anti-HA signals. Scale bars = 20 μm long. The GTP-locked form is myc-Rab2(Q65L).

Table 1. TEM-β-lactamase RicA translocation assay.

B. abortus strain	Fusion produced	Percentage of infected cells CCF2 positive[a]	Number of infected cells examined
Wild type	TEM-β-lactamase	0.2	542
Wild type	TEM-β-lactamase-RicA	11.2	614
Δ*virB*	TEM-β-lactamase-RicA	0.7	697
Wild type	TEM-β-lactamase-VceA	7.4	231

a. Infected cells CCF2 are supposed to be detected as positive when TEM-β-lactamase is translocated to the host cell cytoplasm.

tested were RAW264.7 macrophages. In these experiments, the non-infected cells were almost always negative (> 99%), i.e. in the background of fluorescence. We counted the proportion of infected cells that were positive for β-lactamase activity. In agreement with previously reported results (de Jong *et al*., 2008), the TEM-β-lactamase-VceA was translocated to RAW264.7 macrophages at 16 h post infection (p.i.) (Table 1). The TEM-β-lactamase-RicA fusion was also detected as translocated in the same conditions (a representative image is shown in Fig. 3), while the TEM-β-lactamase was not (Table 1). Interestingly, when TEM-β-lactamase-RicA was tested in a *B. abortus* Δ*virB* mutant, i.e. a strain in which the complete *virB* operon is deleted, the level of translocation was very low, similar to the negative control (Table 1). At least two interpretations of this observation are possible. First, the TEM-β-lactamase-RicA fusion would be translocated by the T4SS, and second, the Δ*virB* trafficking being altered, the mutant bacteria would be located within compartments in which translocation (by another secretion system) is not functional.

To determine if RicA was secreted in bacteriological culture, translational fusions with a 3Flag tag at the N-terminus or at the C-terminus were generated (expressed from pDF34 or pDF35 plasmids, respectively). The plasmids carrying these fusions were introduced in the *B. abortus* 2308 wild-type strain. After growth in a defined medium, the presence of 3Flag fusions in the bacterial pellets as well as in the concentrated culture supernatants, were assessed by Western

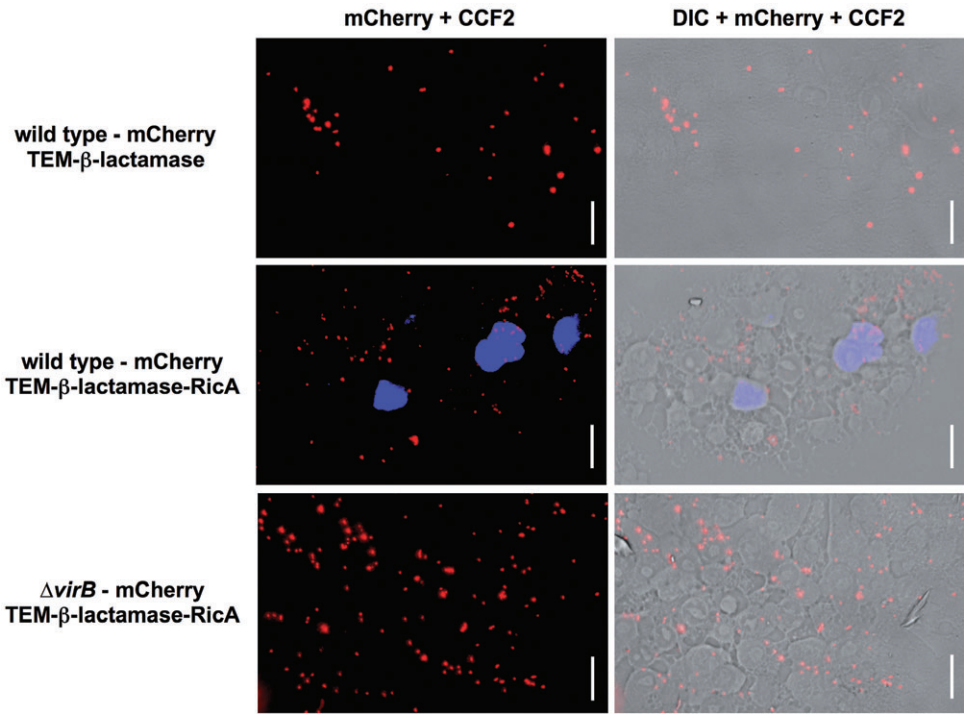

Fig. 3. TEM-β-lactamase-RicA translocation into RAW264.7 macrophages. Bacteria are labelled by constitutively produced mCherry (red), and β-lactamase activity is detected using CCF2 (blue) fluorescence. Scale bars = 20 μm long. The mCherry and CCF2 signals are shown on the left; these signals are overlaid with DIC on the right panels. A fraction of the infected cells are CCF2-positive (see Table 1 for countings). The TEM-β-lactamase-RicA translocation was tested in either wild type of Δ*virB B. abortus* strain. Despite high multiplicity of infection with the Δ*virB* strain, no translocation of TEM-β-lactamase-RicA could be detected with this strain. A representative image is shown for each tested condition.

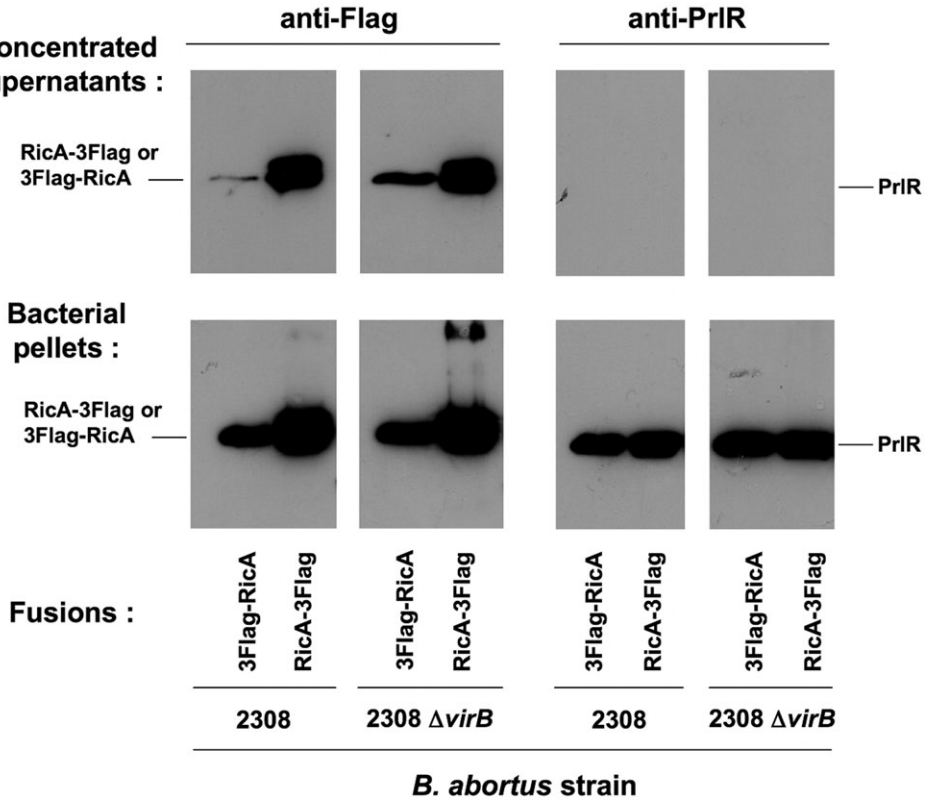

Fig. 4. VirB-independent secretion of 3Flag-RicA by *B. abortus*. Western blots were carried out on concentrated culture supernatants (upper part) or bacterial pellets (lower part), using either the M2 anti-Flag monoclonal antibody (anti-Flag, left part) or polyclonal anti-PrlR antibodies (anti-PrlR, right part). PrlR detection was used as a control for lysis. The expected distances of migration for RicA-3Flag, 3Flag-RicA and PrlR are indicated.

blot using the M2 anti-Flag antibody. The tagged forms of RicA were detected at their expected molecular mass in the bacterial pellets (Fig. 4) suggesting that they were expressed and stable. The 3Flag-RicA and RicA-3Flag fusions were also detected in the concentrated supernatant, whereas the cytosolic protein PrlR, used as control, was not (Fig. 4), indicating that these fusions are indeed secreted and do not result from a lysis of the bacteria. The fact that both fusions are secreted in the culture medium suggests that N-terminal or C-terminal tagging with 3Flag did not alter the secretion signal in the RicA protein.

To determine if 3Flag-RicA or RicA-3Flag secretion was dependent on the VirB T4SS, the same experiment was performed with a *B. abortus* 2308 Δ*virB* strain. The results show that 3Flag-RicA and RicA-3Flag secretion is maintained in the Δ*virB* mutant, in the absence of detectable lysis (Fig. 4). Consequently VirB T4SS is not required for secretion of RicA fusions in the culture medium, suggesting that another unknown secretion system is functional in these conditions. The secretion of RicA-3Flag was also tested in a *B. abortus* Δ*fliF* strain. The *fliF* gene putatively encodes a basal protein of a flagellar structure (Fretin *et al*., 2005), which could be used as a secretion machinery, as reported for *Yersinia enterocolitica* (Young *et al*., 1999). However, the RicA-3Flag secretion is still detected in the Δ*fliF* strain (Fig. 5).

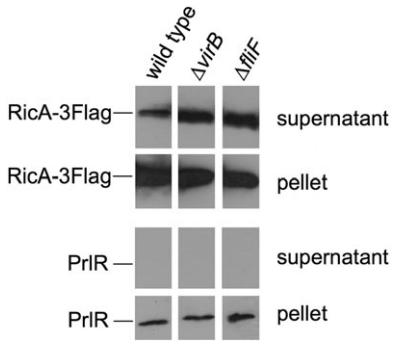

Fig. 5. Secretion of RicA-3Flag from a *B. abortus* Δ*fliF* strain. RicA-3Flag was detected using the M2 anti-Flag antibody, and PrlR was detected using a polyclonal rabbit anti-PrlR serum. The expected migration distances of RicA-3Flag and PrlR are indicated on the left side of the picture. Western blot was performed with culture supernatant concentrated using the PRRM method ('supernatant') or with the bacterial pellet ('pellet').

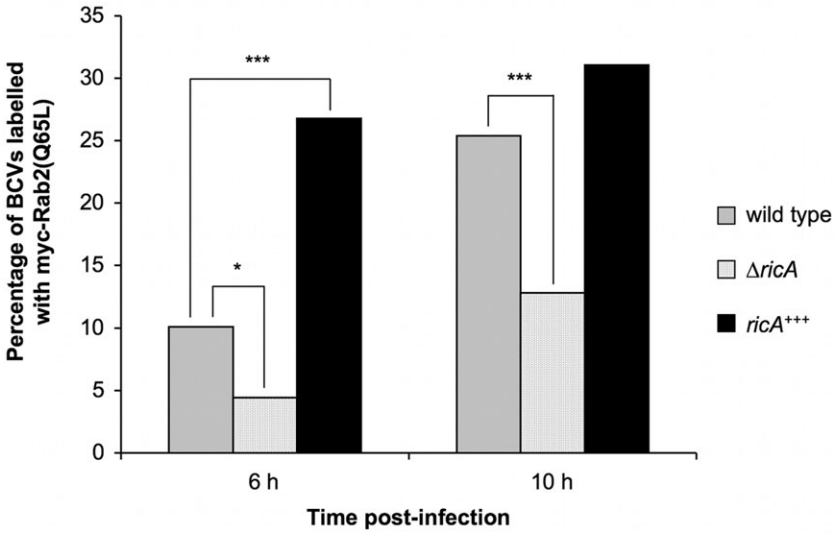

Fig. 6. Recruitment of myc-Rab2(Q65L) on BCVs is impaired by the *ricA* mutation. HeLa cells were transfected with a plasmid allowing the production of GTP-locked myc-Rab2(Q65L), and then infected for 6 or 10 h with a *B. abortus* strain. Three *B. abortus* strains were used, either wild type, Δ*ricA* mutant or a strain overexpressing *ricA* (*ricA*$^{+++}$). Statistical analysis (*t*-test for independent samples) was performed and significant differences are labelled with *($P < 0.05$) or ***($P < 0.001$).

The ricA *deletion does not dramatically impair intracellular replication but alters Rab2 recruitment on BCVs*

An in-frame deletion mutant was first constructed for the *ricA* coding sequence (CDS) in *B. melitensis* 16 M strain. The virulence of the mutant strain was similar to the wild-type strain, when estimated by counting the number of colony forming units (CFU) in the spleen of mice 1 or 4 weeks p.i. (data not shown). Infection of cultured immortalized bovine macrophages or HeLa epithelial cells did not show any significant and reproducible difference between the *B. melitensis ricA* mutant and the wild-type strain, as evaluated by CFU counting. Because the *B. abortus* 2308 strain is the reference for the intracellular trafficking studies, the same *ricA* deletion was also performed in this strain, and it also resulted in the absence of virulence attenuation compared with the wild-type control in HeLa cells (CFU countings at 2, 6, 12, 18, 24 and 48 h p.i., data not shown). Both wild type and Δ*ricA* mutant infected about 9% of HeLa cells at 24 h p.i. (data not shown). These data suggest that there is no major alteration of the internalization, intracellular survival and proliferation inside HeLa cells.

Because RicA is translocated to the host cell during infection, and because it interacts with Rab2, we were interested to test the myc-Rab2 subcellular localization during HeLa cell infection. Indeed, it was previously reported that a GTP-locked form of myc-Rab2 was colocalizing with wild-type BCVs in HeLa cells (Fugier *et al.*, 2009). HeLa cells were first transfected with a plasmid allowing production of GTP-locked myc-Rab2(Q65L), infected with either wild type or Δ*ricA B. abortus* strain for 6 or 10 h, and then fixed. Immunofluorescence was used to specifically detect bacteria and myc fusions, and the number of BCV positive or negative for an anti-myc signal was counted. For the wild-type strain, the percentage of BCVs positive for myc-Rab2(Q65L) increased from 6 to 10 h p.i. in HeLa cells (Fig. 6). This percentage was significantly lower for the Δ*ricA* mutant at both times p.i., while it was significantly higher in a strain overexpressing *ricA* from pDF35, a medium copy plasmid derived from pBBR1 (Antoine and Locht, 1992) (Fig. 6). These data suggest that RicA is able, directly or indirectly, to control the recruitment of active (GTP-bound) Rab2 to the BCVs in HeLa cells.

The intracellular trafficking of a B. abortus ricA *mutant is altered*

Because Rab2 was proposed to be involved in the control of intracellular trafficking of BCVs (Fugier *et al.*, 2009), we followed the colocalization of *B. abortus* Δ*ricA* mutant and the wild-type strain with LAMP1, a marker of late endosomes/lysosomes, in HeLa cells using confocal microscopy after immunolabelling. As previously shown (Pizarro-Cerda *et al.*, 1998), the characteristic trafficking of the *B. abortus* 2308 strain involved the early acquisition of LAMP1 on the BCVs, followed by a slow decrease. As expected, a *virB9* mutant strain unable to replicate in mammalian cells (Celli *et al.*, 2005) conserved the LAMP1 labelling on its BCV (Fig. 7). A statistically significant and reproducible stronger decrease of LAMP1 on Δ*ricA* BCVs was observed, compared with the wild-type strain (Fig. 7). When a plasmid bearing *ricA* (pDF40) was introduced in the *B. abortus* Δ*ricA* strain, the fraction of BCVs labelled with LAMP1 (26%, 74 LAMP1 positive BCVs out of 290 BCVs) at 12 h p.i. was significantly higher ($\chi^2 < 0.001$) compared with the Δ*ricA* strain (13%, 29 LAMP1 positive BCVs out of 228

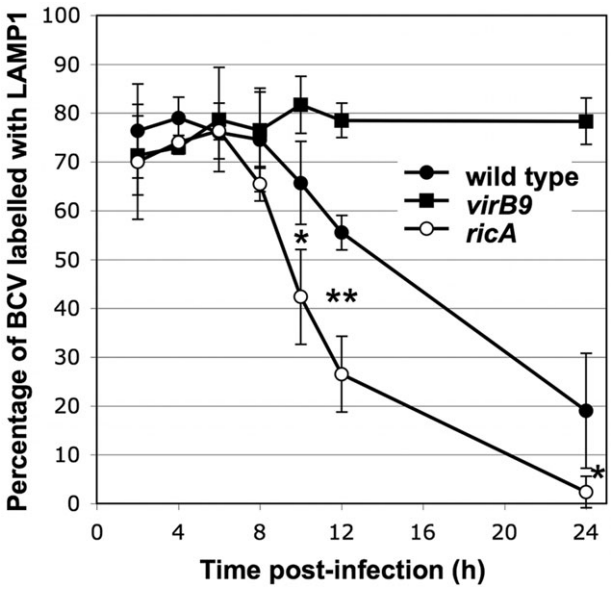

Fig. 7. Trafficking of *B. abortus* 2308 and its Δ*ricA* and *virB9* isogenic mutants. HeLa cells infected with wild-type *B. abortus*, Δ*ricA* mutant and *virB9* mutant were fixed at different time points of the infection. The percentage of wild type, Δ*ricA* or *virB9* mutant-containing vacuoles retaining LAMP1, a marker of late endosome, was scored using immunofluorescence microscopy. Data are means ± standard deviations of three independent experiments. The difference between wild-type strain and Δ*ricA* mutant is statistically significant ($P < 0.05$ or $P < 0.01$ for comparisons indicated by '*' or '**', respectively) according to a *t*-test for independent samples. Complementation of the Δ*ricA* mutant *in trans* is described in the main text.

BCVs). The wild-type strain displayed an even higher percentage of LAMP1-positive BCVs (37%, 69 LAMP1 positive BCVs out of 185 BCVs) at the same time p.i., showing that complementation is partial. The LAMP1 loss on BCVs containing Δ*ricA* strain suggests that these BCVs loose late endosomal markers earlier than the wild-type strain. At later times during the infection, the BCVs containing Δ*ricA* strain were labelled with the calnexin ER marker like the wild-type BCVs (data not shown), suggesting that both strains replicate in the ER.

A careful examination of the infected cells at 24 h p.i. immunostained for *B. abortus* lipolysaccharide allowed the observation of a higher number of *ricA* mutants per infected cell (Fig. 8C,D,G), compared with the wild-type strain (Fig. 8A,B,G) at 24 h p.i. This was unexpected as CFU/well was not higher for the *ricA* mutant compared with the wild type. This effect was compensated by the expression of *ricA* from a low copy vector (pDF040) (Fig. 8E,F,G), consistent with the full complementation of the *ricA* mutation regarding this phenotype. This further indicates that the earlier intracellular proliferation of the Δ*ricA* mutant is due to the loss of function generated by *ricA* deletion.

Discussion

Several bacterial effectors are found to bind host proteins, and this feature was used to identify putative effectors interacting with a given host protein, like *L. pneumophila* SidM(DrrA) that binds to Rab1 (Machner and Isberg, 2006) or *Salmonella typhimurium* SopE that binds to Cdc42 (Hardt *et al*., 1998). In this report, we undertook an original large-scale screening using a set of human putatively phagosomal proteins, as baits to identify *Brucella* interactors. This kind of approach is feasible thanks to the availability of ORFeomes for human (Rual *et al*., 2004; Lamesch *et al*., 2007) and pathogenic bacteria such as *Pseudomonas aeruginosa* (Labaer *et al*., 2004), *B. melitensis* (Dricot *et al*., 2004), *Staphylococcus aureus* (Brandner *et al*., 2008) or *Mycobacterium tuberculosis* (Wang *et al*., 2010). This screening allowed the identification of RicA, a protein able to specifically interact with the small GTPase Rab2. The interest of this screening procedure is that it could in principle be applied to any pathogen for which a genomic sequence is available.

According to our data, a tagged RicA protein is translocated to RAW264.7 macrophages during infection, but this translocation is not observed from a Δ*virB* mutant (Table 1). A 3Flag-RicA fusion is secreted in bacterial culture medium and this secretion is VirB-independent, as it is still observed in a Δ*virB* mutant (Fig. 4). This is consistent with the absence of obvious type IV secretion signal at the C-terminus of RicA as found for type IV effectors of other α-proteobacteria like AnkA of *Anaplasma phagocytophilum* (Lin *et al*., 2007) or those from *Agrobacterium tumefaciens* (Vergunst *et al*., 2005). VirB-independent translocation suggests that at least one other secretion system is present and active in these conditions, and it also means that translocation to RAW264.7 macrophages could occur by a secretion system that is not T4SS. This unidentified secretion system would be functional in a compartment that is not reached by the Δ*virB* mutant. Translocation of tagged RicA by outer membrane vesicles is unlikely because there is no predicted signal peptide for RicA. Moreover, RicA-3Flag is still secreted in a *B. abortus* Δ*fliF* mutant (Fig. 5), *fliF* being homologous to genes encoding a basal component of the flagellum, indicating that the flagellar apparatus is not involved in RicA secretion, at least in bacterial cultures. The secretion system functional for RicA secretion in the culture medium remains to be discovered, and more data are necessary to clarify the role of T4SS in the translocation to the host cell cytosol.

The interaction of RicA with Rab2 could be relevant in the host cell. It has been recently demonstrated that Rab2 is recruited on the BCVs during infection of BHK-21 and HeLa cell lines (Fugier *et al*., 2009). Moreover, Fugier

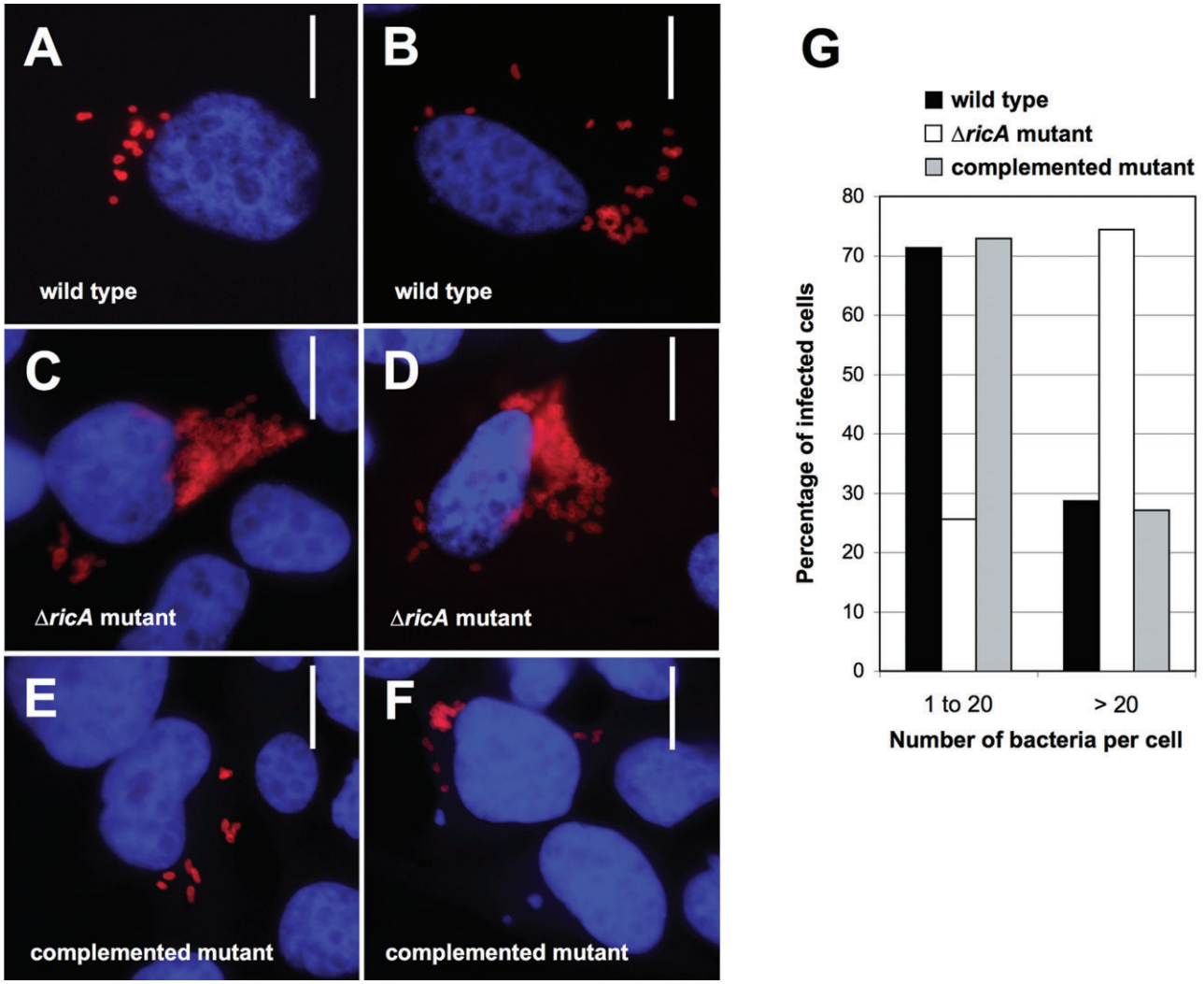

Fig. 8. Replication of wild type and Δ*ricA* mutant in HeLa cells. HeLa cells were infected for 24 h with either wild type, Δ*ricA* and complemented Δ*ricA* mutant. Cells were fixed, bacteria were labelled with a monoclonal A76-12G12 anti-LPS antibody and DNA was labelled with DAPI. Two representative immunofluorescence pictures of HeLa cells infected with *B. abortus* wild-type strain 24 h post infection (A, B), *B. abortus* Δ*ricA* strain 24 h post infection (C, D), complemented *B. abortus* Δ*ricA* strain 24 h post infection (E, F). Scale bars = 10 μm long. (G) The number of bacteria per infected cell was evaluated, and frequencies are reported in two classes according to the number of bacteria per infected cell (< or > 20). The numbers of infected cells scored for wild type, Δ*ricA* and complemented strains were 157, 129 and 133 respectively. The differences between wild type and Δ*ricA* mutant, and between Δ*ricA* mutant and the complementation strain, were statistically significant ($P < 0.001$) according to a χ^2 test.

et al. also demonstrated that functional Rab2 is necessary for a successful *B. abortus* cellular infection because production of a GDP-locked form of Rab2 leads to a decrease of *B. abortus* replication, and blocks the bacterium in late endosomal compartments (Fugier *et al*., 2009). Our data (Fig. 6) strongly suggest that RicA could contribute to Rab2 recruitment on the BCVs, but the precise mechanism of this recruitment and its role during intracellular infection is unclear. Preferential interaction of RicA with the GDP-bound Rab2 suggested that RicA could act as a GEF for Rab2, but biochemical data reported here do not support this hypothesis. The role of RicA could be to bind GDP-Rab2 in the cytosol or at the cellular membranes to help its recruitment to the BCV. In this case, RicA could be considered as a GDI or a REP (Rab escort protein). It is well known that Rab GTPase function can be manipulated by bacterial pathogens (Brumell and Scidmore, 2007). Actually, the pattern of recruitment of Rab GTPases to the bacterium containing vacuoles could be complex. Indeed, up to 18 different Rab GTPases were found to be associated to *Salmonella enterica*-containing vacuoles (Smith *et al*., 2007). In eukaryotic cells, Rab2 is often located to the ER-Golgi intermediate compartments and it was demonstrated to play a role in membrane transport between the Golgi and the ER apparatus (Tisdale *et al*., 1992). Because Rab2

controls recruitment of microtubules and dynein (Tisdale *et al*., 2009), it is possible that BCVs containing a Δ*ricA* mutant traffic differently compared with the BCVs containing a wild-type strain because their association to microtubules and/or their mobility along microtubules are affected. However, it was also observed that Rab2 may be associated with purified phagosomes (Garin *et al*., 2001; Stuart *et al*., 2007) and that a Rab2 homologue in *Caenorhabditis elegans* plays a role in the fusion of lysosomes with phagosomes involved in apoptotic cells removal by engulfing cells (Mangahas *et al*., 2008). It is therefore possible that Rab2 is also involved in phagosome maturation in mammalian cells. The observation of a significant reduction of LAMP1 immunodetection on BCVs at intermediate time points (10–12 h p.i.) suggests that RicA could be directly or indirectly involved in BCV maturation, perhaps by modulating the kinetics of BCV maturation by acting on Rab2. The earlier loss of LAMP1 labelling correlates with the enhanced Δ*ricA* proliferation at 24 h p.i. In the natural infection context, RicA could have been selected because of its role in the intracellular trafficking control, or the modulation of the host immune response. For example, Rab2b was found to modulate the production of exosomes (Ostrowski *et al*., 2010), previously shown to be involved in communication between immune cells (Thery *et al*., 2002), and therefore a modulation of Rab2 isoenzymes by the pathogen could lead to a modulation of host immune response. These lines of research remain to be investigated.

The predicted tertiary structure of RicA is similar to the one of LpxA (Raetz and Roderick, 1995), an acyltransferase involved in lipopolysaccharide biosynthesis. The 3D model of RicA structure is composed of a left-handed β helix followed by a C-terminal α helix, a classical fold for transferases. In *B. abortus*, RicA is distantly homologous to CysE, a serine acetyltransferase. VipF (Shohdy *et al*., 2005), a *Legionella pneumophila* effector, is also a putative acetyltransferase, but from a different family. Preliminary data do not support an acetyltransferase activity of RicA on Rab2 and GEF assay of His_6-RicA with GST-Rab2 is not enhanced by the presence of acetyl-CoA (data not shown). One particular feature of RicA is that it belongs to a family of well-conserved proteins. This is unusual for bacterial effectors that are generally poorly conserved. Indeed, among the 31 *L. pneumophila* effectors reviewed by Ninio and Roy (Ninio and Roy, 2007), only four are conserved in several bacterial classes. The conservation of RicA homologues in free living bacteria is surprising, suggesting that its function in Rab2 modulation could be a recent acquisition along evolution, maybe because of minor surface changes. A limited access of *Brucella* spp. to horizontal gene pools (Bohlin *et al*., 2010), compared with other more 'social' pathogens like enteric bacteria, could explain why pre-existing mutated proteins would be selected to achieve new functions related to virulence.

Experimental procedures

Bacterial and yeast strains

All *Brucella* strains used in this study (Table 2) were derived from *B. melitensis* 16 M or *B. abortus* 2308 Nal^R (spontaneous nalidixic acid resistant mutant), and were routinely cultivated in 2YT rich medium (1% yeast extract, 1.6% peptone, 0.5% NaCl) or Tryptic Soy Broth respectively. A specific culture medium was used for secretion tests (see below). *Escherichia coli* strains used for molecular cloning experiments were DH10B (Invitrogen) and DB3.1 (Invitrogen). All *E. coli* strains were grown in Luria–Bertani (LB) broth. Antibiotics were used at the following concentrations when appropriate: nalidixic acid, 25 μg ml^{-1}; kanamycin, 20 μg ml^{-1}; chloramphenicol, 20 μg ml^{-1}; ampicillin (Amp), 100 μg ml^{-1}; gentamicin, 50 μg ml^{-1}. Plasmids (Table 2) were mobilized from *E. coli* strain S17-1 (Simon *et al*., 1983) into *B. melitensis* or *B. abortus* by bacterial conjugation. Yeast growth media and genetic techniques have been previously described (Sherman, 1991).

HT-Y2H

The *B. melitensis* ORFeome v1.1 has been described previously (Dricot *et al*., 2004). It is constituted by 3091 Gateway entry clones organized into 35 96-well plates, each plate containing a maximum of 94 ORFs. Position in the ORFeome plates is based on the size of the ORFs on the two chromosomes of *B. melitensis*. Plasmids of the *B. melitensis* ORFeome were prepared using NucleoSpin Robot 96 Core Kit (Macherey-Nagel) and a NucleoVac 96 Vacuum Manifold (Macherey-Nagel). DNA concentration was evaluated from agarose gel and plasmids were grouped into small pools (half a plate of the ORFeome per pool) giving 71 mini-pools, each containing between 5 and 48 different ORFs, with similar plasmid concentration per ORF.

The 71 mini-pools were transferred individually by Gateway recombinational cloning (Walhout *et al*., 2000) into pAD-dest-CYH destination vector (Walhout *et al*., 2000) to generate 71 pools of AD-ORF fusions. Products from recombinational cloning reactions were used to transform ultra electro competent *E. coli* cells (ElectroMAX DH10B strain, Invitrogen). The 71 transformations were then individually plated onto LB + Amp plates in order to obtain at least 10^5 individual colonies per transformation. Colonies of each transformation were then resuspended into LB + Amp liquid medium. Half of the mix was stored in 50% glycerol, the other part was used to prepare 71 AD-ORF mini-pools of destination plasmids.

For yeast transformation, the 71 AD-ORF mini-pools of destination plasmids were transformed individually into *MAT*a MaV103 yeast strain (Vidal *et al*., 1996). Transformed cells were individually plated on solid synthetic complete (Sc) media lacking tryptophan (Sc-W) (Walhout and Vidal, 2001). Growing colonies (> 10^5 individual colonies per transformation) were then resuspended in liquid Sc-W medium and stored with 20% glycerol for subsequent use. Aliquots of AD-ORF transformed yeast cells were pooled to generate 19 mini-libraries each containing a maximum of 188 individual AD-ORF transformants as described previously (Rual *et al*., 2005).

Table 2. Strains and plasmids.

	Description	Reference or source
Strain		
B. abortus strains		
2308	wild type	
MDB001	Δ*virB* in 2308	This study
AJ002	Δ*ricA* in 2308 strain	This study
B. melitensis strains		
16 M	wild type	A. P. MacMillan
AJ001	Δ*ricA* in 16 M strain	This study
E. coli strains		
DH10B	Cloning strain	Invitrogen Life-Technologies
DB3.1	*ccdB* resistant cloning strain	Invitrogen Life-Technologies
S17-1	RP4-2, Tc::Mu,Km-Tn7, for plasmid mobilization	Simon *et al.* (1983)
BL21(DE3)	An *E. coli* B strain with DE3, a λ prophage carrying the T7 RNA polymerase gene and *lacI*^{q}	Novagen
AJ101	pGEX-2TK in BL21(DE3)	This study
AJ102	pAJ102 in BL21(DE3)	This study
DF101	pDF34 in DH10B	This study
Plasmids		
pDONR201	BP cloning vector	Invitrogen Life-Technologies
pGEX-2TK	GST fusion vector	GE Healthcare
pGEM-T Easy	Vector for PCR fragments cloning	Promega
pGEM-T-Δ*ricA*	Intermediary construct for ricA deletion	This study
pJQ200uc1	Plasmid allowing allelic exchange	Quandt and Hynes (1993)
pBBR1MCS	Medium-copy broad host range plasmid	Kovach *et al.* (1994)
pMR10*cat*	Low-copy plasmid (RK2*oriV*)	C. D. Mohr and R. C. Roberts[a]
pET15b	Overexpression vector with T7 promoter for His_6-fusion	Novagen
pJQΔ*ricA*	Plasmid allowing *ricA* deletion	This study
pET15b-RicA	His_6-RicA overproduction plasmid	This study
pV1899	pGateway 5′ CMV5-Triple Flag (Nterm)	Braun *et al.* (2009)
pV1900	pGateway 3′ CMV5-Triple Flag (Cterm)	Braun *et al.* (2009)
pV1899-ricA	pV1899 carrying *ricA* CDS	This study
pV1900-ricA	pV1900 carrying *ricA* CDS	This study
pMDB001	Gateway-compatible 3Flag medium copy vector	This study
pMDB002	3Flag Gateway-compatible medium copy vector	This study
pDF08	pDONR201 carrying *ricA* coding sequence (CDS)	This study
pAJ102	pGEX-2TK carrying *rab2* CDS	This study
pDF40	pMR10*cat* carrying *ricA* with its promoter	This study
pDF34	pBBR1MCS expressing 3Flag-RicA	This study
pDF35	pBBR1MCS expressing RicA-3Flag	This study
pFlagTEM1	β-lactamase reporter cloning vector	Raffatellu *et al.* (2005)
pFlagTEM1_vceA	pFlagTEM1 expressing *vceA*	de Jong *et al.* (2008)
pFlagTEM1-ricA	pFlagTEM1 expressing *ricA*	This study
pCMV-HA-GW	pCMV-HA (Clontech) Gateway-compatible	S. Méresse[a]
pCMV-HA-ricA	pCMV-HA-GW carrying *ricA* CDS	This study

a. Unpublished.

The 96-well format process designed and described by Rual and colleagues (Rual *et al.*, 2005) was used to mate 221 individual *MAT*α MaV203 DB-ORF yeast strains (human baits cherry-picked from the CCSB human ORFeome collection, a complete list is available in Table S1) with the 19 mini-libraries each containing a maximum of 188 individual *MAT*a MaV103 AD-ORF transformants (*Brucella* preys). Each DB-ORF was individually mated to each of the 19 AD-ORFs mini-libraries on YEPD (yeast extract 10 g l^{-1}, peptone 20 g l^{-1} and dextrose 20 g l^{-1}) solid medium, representing about 680 000 combinations. After overnight growth at 30°C, colonies were transferred to Sc-L-W-H+3AT plates (lacking leucine, tryptophan, histidine and containing 20 mM 3-Amino-1,2,4-triazole) to select for diploids that exhibited elevated expression levels of the *GAL1::HIS3* yeast two-hybrid reporter (Walhout and Vidal, 2001). This first phenotypic screen yielded ~300 positive colonies, which were transferred in parallel onto Sc-L-H+3AT+CYH plates (lacking leucine, histidine and containing 20 mM 3-AT, tryptophan and 1 μg ml^{-1} cycloheximide) to identify the auto-activators that can arise during yeast two-hybrid selections (Vidalain *et al.*, 2004). The plates were incubated overnight at 30°C and replica-clean with sterile velvets as if the plates needed to be replica-plated (Walhout and Vidal, 2001), this step allows to dilute out the yeasts present in each spot and to eliminate non-specific growing. The plates were then incubated at 30°C, 3–5 days and 172 potential positives candidates were picked. Polymerase chain reaction (PCR) amplifications and sequencing of DB-ORF and AD-ORF fragments allowed generation of 144 pairs of interaction sequence tags (a complete list is available in Table S2). Redundant pairs of interaction sequence tags and three humans proteins considered as sticky proteins [annotated as syndecan binding protein (syntenin) 2,baculoviral IAP repeat-containing 4, baculoviral IAP repeat-containing 2] were eliminated. This resulted in a set of 38 *Brucella*–human Y2H interactions.

Construction of RicA fusions to 3Flag tag

pDF34 plasmid expressing 3Flag-RicA used for secretion assays and for the pull-down assay was constructed as follows. The *ricA* CDS was amplified using primers A (5′-caagcttccgatctatgca-3′) and B (5′-cggatcctcaggcaggctccatgc-3′) and introduced into pV1899-Gateway 5′CMV 3Flag (Braun *et al*., 2009) digested by BamHI and HindIII to fuse *ricA* CDS with the 3Flag tag. The *3flag-ricA* fragment was then amplified using primers C (5′-ctggtaccttgaaggaaacagctatggactacaaagac-3′) and B, digested with Asp718I and BamHI and cloned in pBBR1MCS opened using the same restriction enzymes, giving pDF34.

To produce RicA with C-terminal 3Flag, *ricA* sequence was amplified using primers D (5′-tggtaccatgatgaaggaaacagctatgc cgatctatgca-3′) and E (5′-gtctagaggcaggctccatgccgc-3′) with pDF08 as template and then inserted in pV1900-*rab2* digested by Asp718I and XbaI. The resulting *ricA*-3Flag fusion was extracted from the vector using Asp718I and BamHI and cloned in pBBR1MCS opened with the same restriction enzymes giving pDF35.

GST and GST-Rab2 overproduction and purification

GST and GST-Rab2 were produced from AJ101 and AJ102 strains respectively. A culture at an OD_{600} of 0.7 was induced with 1 mM IPTG at 30°C for 8 h. Cells were collected after centrifugation at 4200 *g* for 5 min in pre-chilled tubes, resuspended in binding buffer [PBS, 10 mM $MgCl_2$, 0.05% Tween 20, 10% Glycerol, EDTA-free Complete antiprotease cocktail (Roche Cat. No. 11697498001)] and sonicated on ice (3 cycles of 30 s). Cell debris were separated at 12 000 *g* for 30 min and the supernatant was collected and filtered with 0.45 μm filter into pre-chilled tubes.

Gravity columns (Biorad Cat. No. 732–1010) were used as recommended by the manufacturer, with Uniflow glutathione resin (Clontech Cat. No. 635610), except for the elution step that was replaced by a resuspension of the column content (resin + GST or GST-Rab2) in 1 ml bead storage buffer (see composition in the GST pull-down section) after a washing step in the same buffer. The suspension was collected into a microtube and stored at −20°C.

GST pull-down

A culture of DF101 strain at an OD_{600} of 0.8 was induced with 1 mM IPTG for 4 h at 37°C. Pellet was resuspended in bead storage buffer (see composition below), sonicated 10 cycles of 30 s and spun at 12 000 *g* for 30 min. Supernatant was filtered with a 0.45 μm filter and stored at −20°C.

The GST pull-down was performed following Alternate protocol 1 for effector isolation with GST-tagged small GTPases as previously described (Brymora *et al*., 2004), except for: (i) the bead storage buffer composition, which was 50 mM Tris pH 7.5, 120 mM NaCl, 0.5% NP-40, 10% glycerol, 10 mM $MgCl_2$, EDTA-free Complete antiprotease cocktail, 0.22 μm filtered; (ii) the small GTPase loading buffer composition, which was 20 mM Tris pH 7.4, 25 mM NaCl, 5 mM EDTA; (iii) columns that were replaced by microtubes and (iv) the binding step that was performed overnight.

The proportions of beads-bound GST and GST-Rab2 used in the pull-down were estimated after SDS-PAGE migration and Coomassie staining. GDP and GTPγS were from Sigma (Cat. No. G7127 and G8634, respectively). Final samples were submitted to Western blotting for the detection of 3Flag-RicA, GST and GST-Rab2.

GDP/GTP exchange (GEF) assay

The GEF assay was performed with purified GST-Rab2 and purified His_6-RicA. The purification methods and the GEF assay are described below.

GST-Rab2 purification. GST-Rab2 purification was performed as described above, except that 10 mM $MgCl_2$ and 1 mM GDP were added to the binding buffer, and that 1 mM $MgCl_2$ and 0.1 mM GDP were added to the elution buffer. GST-Rab2 was eluted from the beads by adding 10 mM glutathion.

His6-RicA overproduction and purification. His_6-RicA fusion was produced from a BL21(DE3) strain transformed with pET15b-RicA, a pET15b vector (Novagen) with the *ricA* (BMEI0736) coding sequence inserted at NdeI-BamHI restriction sites. A culture at an OD_{600} between 0.6 and 0.8 was induced with 1 mM isopropyl-β-D-thiogalactoside (IPTG) at 37°C for 3 h. The cells were harvested by centrifugation at 4200 *g* for 5 min at 4°C. Pellet was resuspended in 4 ml of binding buffer (45 mM Tris-HCl pH 7.9, 500 mM NaCl, 5 mM imidazole, 10% glycerol and EDTA-free Complete antiprotease cocktail, Roche, Cat. No. 11697498001) and sonicated on ice (10 cycles of 30 s). Cell debris were collected by centrifugation at 12 000 *g* for 30 min at 4°C. The supernatant was filtered with 0.45 μm filter into pre-chilled tubes and transferred into a chromatography column (Biorad, Econo-Pac cat. No. 732–1010) preloaded with 1.2 ml Ni-NTA His Bind resin (Novagen, Cat. No. 70691–3). After a 1 h incubation at 4°C, the column was washed several times with a buffer containing 20 mM Tris-HCl pH 7.9, 150 mM NaCl and antiprotease cocktail. His_6-RicA was eluted with 50 mM EDTA in 20 mM Tris-HCl pH 7.9, 150 mM NaCl and antiprotease cocktail. His6-RicA was desalted by two passages on Microcon filter unit with a 10 kDa cut-off (Millipore, Cat. No. 42406), followed by buffer exchange for 20 mM Tris-HCl pH 7.9, 150 mM NaCl and 0.5 mM $MgCl_2$ on NAP5-column (GE Healthcare).

GEF assay. GST-Rab2 was loaded with mant-GDP, 1′(3)-bis-O-(N-methylanthraniloyl) GDP (Molecular Probes), a fluorescent GDP analogue, by incubating 0.6 mM of mant-GDP with 6 μM of purified GST-Rab2 for 30 min at 37°C in a loading buffer (20 mM Tris pH 8.0, 150 mM NaCl,5 mM EDTA and 1 mM DTT), as previously reported (Murata *et al*., 2006). The solution was then transferred on ice and 10 mM $MgCl_2$ was added to stop the reaction. The loading buffer was exchanged for the reaction buffer (containing 20 mM Tris pH 8.0, 150 mM NaCl and 0.5 mM $MgCl_2$) using a NAP5-column (GE Healthcare) to remove free mant-GDP. For the nucleotide exchange assay, 3 μM of GST-Rab2 bound to mant-GDP was used. The dissociation of mant-GDP was determined by measuring the decrease of fluorescence corresponding to the release of mant-GDP in presence of 200 μM of GTP, with 3 μM of His_6-RicA. Samples were excited at 360 nm and emission was monitored at 434 nm using a AMINCO-Bowman series 2 (AB2) spectrofluorometer. As a positive control for mant-GDP dissociation from GST-Rab2 was performed using 5 mM of EDTA (and no His_6-RicA). The stability

control for mant-GDP/GST-Rab2 complex was performed in the absence of EDTA and His_6-RicA, in the presence of the elution buffer used for the assay with His_6-RicA.

Transfections for localization of HA-RicA and myc-Rab2 fusions by immunofluorescence

The Gateway destination vector pCMV-HA-GW was a kind gift from Stéphane Méresse. It was constructed by EcoRI digestion of the pCMV-HA (Clontech), fill-in of cohesive ends and blunt-end cloning of the Gateway reading frame cassette A (Invitrogen). The *ricA* CDS was transferred from pDF08 (Table 2) to pCMV-HA-GW using LR recombinational cloning, generating the pCMV-HA-ricA. The pCMV-myc derivatives allowing production of myc-Rab2, myc-Rab2(Q65L) and myc-Rab2(N119I) were previously described (Fugier *et al.*, 2009).

For immunofluorescence microscopy, cells grown on coverslips were fixed in 3% paraformaldehyde in PBS, pH 7.4, at 37°C for 10 min. Fixed cells were washed two times with PBS and permeabilized with 0.1% saponin. Primary and secondary antibodies were diluted, respectively, 1000 and 2000 times in PBS containing 0.1% saponin and 5% horse serum. Coverslips were incubated with primary antibodies for 30 min at room temperature, washed in PBS containing 0.1% saponin and then incubated with appropriate secondary antibodies. Coverslips were mounted onto glass slides using Mowiol 4–88 (Polysciences). Samples were examined and images acquired using a Zeiss LSM510 laser scanning confocal microscope at the Mima2 facilities in Jouy-en-Josas (France). Images of 512×512 pixels were assembled using the image processing package FiJi (http://pacific.mpi-cbg.de/). The primary antibodies used for immunofluorescence microscopy were mouse anti-c-myc IgG1κ (clone 9E10, Roche), or rat anti-HA IgG1 (3F10, Roche). The secondary antibodies were donkey anti-mouse IgG conjugated to Alexa Fluor 488 (Invitrogen), and goat anti-rat IgG conjugated to Alexa Fluor 594 (Invitrogen).

Cellular infections and intracellular trafficking

HeLa cells were inoculated at a multiplicity of infection of 200:1 for microscopy studies. Briefly, bacteria were centrifuged onto cells at 400 *g* for 10 min at 4°C and then incubated for 30 min at 37°C with 5% CO_2 atmosphere. Cells were washed twice with medium and then incubated for 1 h in medium supplemented with 50 μg ml^{-1} gentamicin to kill extracellular bacteria. Thereafter, the antibiotic concentration was decreased to 10 μg ml^{-1}. Cells were then fixed in 3% paraformaldehyde, pH 7.4, at 37°C for 15 min and then processed for immunofluorescence labelling as previously described (Pizarro-Cerda *et al.*, 1998). Samples were examined either on a Leica DMRBE epifluorescence microscope or on a Zeiss LSM 510 laser scanning confocal microscope and more than 100 infected cells were quantified for each strain and time point, in three independent experiments. The primary antibodies used for immunofluorescence microscopy were the following: cow anti-*B. abortus* polyclonal antibody at a dilution of 1/2000; mouse anti-LAMP-1 clone H4A3 (developed by August J. T. and Hildreth E. K., and obtained from the Developmental Studies Hybridoma Bank under the auspices of the NICHD and maintained by the University of Iowa) at a dilution of 1/200 and the rabbit polyclonal anti-calnexin antibody (Stressgen) at a dilution of 1/200. For the counting of *B. abortus* per cells, various strains were used to infect HeLa cells, and infected cells were fixed at 12 or 24 h p.i. as described above. The immunodetection of *B. abortus* was made with A76-12G12 monoclonal antibody (undiluted hybridoma culture supernatant) (Cloeckaert *et al.*, 1993), using a goat anti-mouse IgG antibody coupled to Texas Red diluted to 1/500 (Invitrogen). DAPI (4,6-diamidino-2-phenylindole) staining was made to label DNA, it was incubated (1 μg ml^{-1} final) at the same time as the secondary antibody.

Translocation assay

For translocation assay, 2.10^5 RAW264.7 macrophages were seeded in 12-well plates containing coverslips and infected with *B. abortus* 2308 mCherry expressing TEM1 fusion proteins at a multiplicity of infection of 1000:1. Infections were performed as described above except for IPTG (1 mM) added with medium supplemented with gentamycin 10 μg ml^{-1}. After different time p.i. (4 and 16 h), cells were loaded with a solution containing the fluorescent substrate CCF2/AM at a final concentration of 1 mM for 90 min at room temperature following manufacturer instructions (Invitrogen). Cells were washed two times with PBS and coverslips were inverted on agarose pads (PBS agarose 1%) for fluorescence analysis using Nikon i80 microscope with CCF2 filter set (Chroma).

Sample preparation for secretion test in bacteriological culture medium

Exponentially growing *B. abortus* cells pre-cultured in 2YT were used to inoculate 10 ml of defined medium sterilized by filtration at an OD_{600} of 0.1. *B. abortus* strains were then grown for 24 h. Defined medium composition was the following: $K_2HPO_4.3H_2O$ (9.2 g l^{-1}), KH_2PO_4 (3 g l^{-1}), $N_2S_2O_3$ (0.1 g l^{-1}), NaCl (5 g l^{-1}), Nicotinate (0.2 g l^{-1}), Thiamine (hydrochloride) (0.2 g l^{-1}), Pantothenate (0.07 g l^{-1}) $(NH_4)_2SO_4$ (0.5 g l^{-1}), $MgSO_4$ (10 mg l^{-1}), $MnSO_4$ (0.1 mg l^{-1}), $FeSO_4$ (0.1 mg l^{-1}), Biotine (0.1 mg l^{-1}); and erythritol 2 g l^{-1} as the carbon source. Bacterial pellet and supernatant were separated by centrifugation (3300 *g*, 15 min). Proteins from bacterial culture supernatants were precipitated using the pyrogallol red-molybdate-methanol method (Caldwell and Lattemann, 2004). Concentrated supernatant pellets were resuspended in 20 μl of Laemmli buffer before the Western blot analysis. Bacterial pellets were resuspended in 1 ml of PBS and warmed at 80°C during 1 h. Laemmli buffer was added to obtain an OD_{600} of 5.0 before the Western blot analysis.

Construction of the B. melitensis *and* B. abortus ΔricA *and* ΔvirB *mutants*

Molecular cloning techniques and gel electrophoresis were performed as described previously (Sambrook and Russel, 2001). To construct the deletion mutant of *ricA* in *B. melitensis* and *B. abortus*, upstream and downstream regions flanking *ricA* were amplified by PCR using *B. melitensis* 16 M genomic DNA as template, and the following primer pairs: (i) *ricA*up1 (5′-atggaccagatgctgggtgac-3′) and *ricA*up2 (5′-ggaattctgcagatcttcgatcggcatatgatttctccca-3′); (ii) *ricA*down1 (5′-gaagatctgcagaattccatggagcctgcctgaaaggcg-3′) and *ricA*down2 (5′-cgacatcagggcttgaatgcg-

3′). A second PCR using *ricA*up1 and *ricA*down2 permitted the association of the two PCR products. The resulting fragment was cloned in pGEM-T Easy (Promega Corporation) to generate pGEM-T-Δ*ricA* vector. A NotI fragment containing the region of the *ricA* gene with the deletion of its coding sequence was isolated from pGEM-T-Δ*ricA* and cloned into NotI-cut pJQ200-uc1 (Quandt and Hynes, 1993), generating a new vector named pJQΔ*ricA*. The resulting plasmid was mobilized from *E. coli* S17-1 λ*pir* strain as the donor (Simon *et al*., 1983) to *B. melitensis* 16 M or *B. abortus* 2308 in which it cannot replicate. The allelic replacement strategy was then followed as previously described (Mignolet *et al*., 2010). The *B. abortus* Δ*virB* mutant was constructed as previously described for *B. melitensis* 16 M, using the same plasmid (Nijskens *et al*., 2008).

Construction of the ricA *complementation plasmid*

The *ricA* gene was amplified by PCR using primers hybridizing 237 bp upstream (5′-atctcgagttccatccggagagggcg-3′) and 73 bp downstream (5′-atctgcagccaccgcaagcctcggca-3′) the *ricA* coding sequence. The PCR product was inserted in pGEM-T, and a clone with the expected sequence was ligated into the low copy plasmid pMR10*cat* digested with XhoI and PstI restriction enzymes, placing the *ricA* gene in opposite direction compared with the *lac* promoter of pMR10*cat*. This low copy plasmid carrying the *ricA* gene was called pDF40, and it was mobilized in *B. abortus* Δ*ricA* strain (MDB001) using the S17-1 *E. coli* strain.

Western blotting

Proteins were separated by SDS-PAGE on a 12% polyacrylamide gel before transfer on a nitrocellulose membrane. Membranes were blocked overnight in PBS with 5% non fat dry milk as blocking agent, then incubated 1 h with the primary antibody (diluted in PBS-1% blocking agent), washed three times for 10 min in PBS-0.05% Tween 20, incubated 1 h with the secondary antibody (diluted in PBS-1% blocking agent) and finally washed three times for 10 min in PBS-0.05% Tween 20. Membranes were revealed with ECL (100 mM Tris-HCl pH 8.5, 0.009% H_2O_2, 0.2 mM coumaric acid and 1.25 mM luminol). Primary antibodies used in this study were monoclonal mouse anti-Flag M2 antibody (Sigma Cat. No. F1804, 1:1000 and 1:5000 dilutions for secretion test and GST pull-down experiments, respectively), monoclonal mouse anti-GST (Sigma G1160, 1:10000 dilution for the GST pull-down experiment), and polyclonal rabbit anti-PrlR (home-made, 1:1000). Secondary antibodies were sheep anti-mouse IgG, HRP-linked whole antibody (Amersham Cat. No. NA931, 1:5000 dilution) and donkey anti-rabbit IgG, HRP-linked whole antibody (Amersham Cat. No. NA934, 1:5000 dilution).

Transfection and infection

HeLa cells were transfected with a plasmid allowing production of myc-Rab2(Q65L) (Fugier *et al*., 2009) using Fugene 6 transfection reagent, according to manufacturer instructions (Roche). Transfections were performed 24 h before *Brucella* infection at a multiplicity of infection of 3000:1. At 6 or 10 h p.i., cells were fixed as described above. The immunodetection of myc-Rab2(Q65L) and *Brucella* were performed with an anti-c-myc 9E10 mouse monoclonal antibody diluted 1000 times, and rabbit anti-*B. abortus* polyclonal antibody at a dilution of 1/2000. Secondary antibodies were goat anti-mouse IgG coupled to Alexa 546 and donkey anti-rabbit IgG coupled to Alexa 488, both diluted 500 times.

Acknowledgements

We thank Bruno Goud for his advices about GEF assays with GST-Rab2, Nicolas Lapaque for his advices, helpful discussion and help about immunofluorescence, Rose-Marie Genicot for her technical help, and Sophie Le Blastier for advices about culture supernatant concentration using pyrogallol red-molybdate-methanol. We also thank Stéphane Méresse for providing the pCMV-HA-GW vector. The confocal microscope platforms MIMA2 (Microscopie et imagerie des Microorganismes, Animaux et and URBC (Unité de Recherche en Biologie Cellulaire, University of Namur) are acknowledged. Noelle Ninnane and Catherine Demazy are acknowledged for their technical help regarding confocal microscopy. Funding sources were Communauté Française de Belgique (Action de Recherches Concertées 04/09–325 and 08/13–015), the Fonds pour la Recherche Scientifique-Fonds National pour la Recherche Scientifique (FRS-FNRS, FRFC Grants 2.4521.04 and 2.4541.08), the Ellison Foundation (awarded to Marc Vidal), Institute Sponsored Research from the DFCI Strategic Initiative in support of CCSB, and the University of Namur (FUNDP). We also thank the ‘Fonds pour la formation à la Recherche dans l’Industrie et dans l’Agriculture’ (FRIA) and the FRS-FNRS for PhD thesis fellowships held by M. de Barsy and G. Laloux respectively.

References

Anderson, T.D., and Cheville, N.F. (1986) Ultrastructural morphometric analysis of *Brucella abortus*-infected trophoblasts in experimental placentitis. Bacterial replication occurs in rough endoplasmic reticulum. *Am J Pathol* **124:** 226–237.

Antoine, R., and Locht, C. (1992) Isolation and molecular characterization of a novel broad-host-range plasmid from *Bordetella bronchiseptica* with sequence similarities to plasmids from gram-positive organisms. *Mol Microbiol* **6:** 1785–1799.

Bohlin, J., Snipen, L., Cloeckaert, A., Lagesen, K., Ussery, D., Kristoffersen, A.B., and Godfroid, J. (2010) Genomic comparisons of *Brucella* spp. and closely related bacteria using base compositional and proteome based methods. *BMC Evol Biol* **10:** 249.

Brandner, C.J., Maier, R.H., Henderson, D.S., Hintner, H., Bauer, J.W., and Onder, K. (2008) The ORFeome of *Staphylococcus aureus* v 1.1. *BMC Genomics* **9:** 321.

Braun, P., Tasan, M., Dreze, M., Barrios-Rodiles, M., Lemmens, I., Yu, H., *et al*. (2009) An experimentally derived confidence score for binary protein-protein interactions. *Nat Methods* **6:** 91–97.

Brumell, J.H., and Scidmore, M.A. (2007) Manipulation of rab GTPase function by intracellular bacterial pathogens. *Microbiol Mol Biol Rev* **71:** 636–652.

Brymora, A., Valova, V.A., and Robinson, P.J. (2004) Protein-protein interactions identified by pull-down experiments and mass spectrometry. *Curr Protoc Cell Biol* Chapter 17, Unit 17.5.

Caldwell, R.B., and Lattemann, C.T. (2004) Simple and reliable method to precipitate proteins from bacterial culture supernatant. *Appl Environ Microbiol* **70:** 610–612.

Celli, J., and Gorvel, J.P. (2004) Organelle robbery: *Brucella* interactions with the endoplasmic reticulum. *Curr Opin Microbiol* **7:** 93–97.

Celli, J., de Chastellier, C., Franchini, D.M., Pizarro-Cerda, J., Moreno, E., and Gorvel, J.P. (2003) *Brucella* evades macrophage killing via VirB-dependent sustained interactions with the endoplasmic reticulum. *J Exp Med* **198:** 545–556.

Celli, J., Salcedo, S.P., and Gorvel, J.P. (2005) *Brucella* coopts the small GTPase Sar1 for intracellular replication. *Proc Natl Acad Sci USA* **102:** 1673–1678.

Cloeckaert, A., Zygmunt, M.S., Dubray, G., and Limet, J.N. (1993) Characterization of O-polysaccharide specific monoclonal antibodies derived from mice infected with the rough *Brucella melitensis* strain B115. *J Gen Microbiol* **139:** 1551–1556.

Colicelli, J. (2004) Human RAS superfamily proteins and related GTPases. *Sci STKE* **2004:** RE13.

Comerci, D.J., Martinez-Lorenzo, M.J., Sieira, R., Gorvel, J.P., and Ugalde, R.A. (2001) Essential role of the VirB machinery in the maturation of the *Brucella abortus*-containing vacuole. *Cell Microbiol* **3:** 159–168.

Delrue, R.M., Martinez-Lorenzo, M., Lestrate, P., Danese, I., Bielarz, V., Mertens, P., *et al*. (2001) Identification of *Brucella* spp. genes involved in intracellular trafficking. *Cell Microbiol* **3:** 487–497.

Dricot, A., Rual, J.F., Lamesch, P., Bertin, N., Dupuy, D., Hao, T., *et al*. (2004) Generation of the *Brucella melitensis* ORFeome version 1.1. *Genome Res* **14:** 2201–2206.

Ensminger, A.W., and Isberg, R.R. (2009) *Legionella pneumophila* Dot/Icm translocated substrates: a sum of parts. *Curr Opin Microbiol* **12:** 67–73.

Fretin, D., Fauconnier, A., Kohler, S., Halling, S., Leonard, S., Nijskens, C., *et al*. (2005) The sheathed flagellum of *Brucella melitensis* is involved in persistence in a murine model of infection. *Cell Microbiol* **7:** 687–698.

Fugier, E., Salcedo, S.P., de Chastellier, C., Pophillat, M., Muller, A., Arce-Gorvel, V., *et al*. (2009) The glyceraldehyde-3-phosphate dehydrogenase and the small GTPase Rab 2 are crucial for *Brucella* replication. *PLoS Pathog* **5:** e1000487.

Garin, J., Diez, R., Kieffer, S., Dermine, J.F., Duclos, S., Gagnon, E., *et al*. (2001) The phagosome proteome: insight into phagosome functions. *J Cell Biol* **152:** 165–180.

Hardt, W.D., Chen, L.M., Schuebel, K.E., Bustelo, X.R., and Galan, J.E. (1998) *S. yphimurium* encodes an activator of Rho GTPases that induces membrane ruffling and nuclear responses in host cells. *Cell* **93:** 815–826.

Hemsath, L., and Ahmadian, M.R. (2005) Fluorescence approaches for monitoring interactions of Rho GTPases with nucleotides, regulators, and effectors. *Methods* **37:** 173–182.

de Jong, M.F., Sun, Y.H., den Hartigh, A.B., van Dijl, J.M., and Tsolis, R.M. (2008) Identification of VceA and VceC, two members of the VjbR regulon that are translocated into macrophages by the *Brucella* type IV secretion system. *Mol Microbiol* **70:** 1378–1396.

Kovach, M.E., Phillips, R.W., Elzer, P.H., Roop, R.M., 2nd, and Peterson, K.M. (1994) pBBR1MCS: a broad-host-range cloning vector. *Biotechniques* **16:** 800–802.

Labaer, J., Qiu, Q., Anumanthan, A., Mar, W., Zuo, D., Murthy, T.V., *et al*. (2004) The *Pseudomonas aeruginosa* PA01 gene collection. *Genome Res* **14:** 2190–2200.

Lamesch, P., Li, N., Milstein, S., Fan, C., Hao, T., Szabo, G., *et al*. (2007) hORFeome v3.1: a resource of human open reading frames representing over 10,000 human genes. *Genomics* **89:** 307–315.

Lin, M., den Dulk-Ras, A., Hooykaas, P.J., and Rikihisa, Y. (2007) *Anaplasma phagocytophilum* AnkA secreted by type IV secretion system is tyrosine phosphorylated by Abl-1 to facilitate infection. *Cell Microbiol* **9:** 2644–2657.

Machner, M.P., and Isberg, R.R. (2006) Targeting of host Rab GTPase function by the intravacuolar pathogen *Legionella pneumophila*. *Dev Cell* **11:** 47–56.

Mangahas, P.M., Yu, X., Miller, K.G., and Zhou, Z. (2008) The small GTPase Rab2 functions in the removal of apoptotic cells in *Caenorhabditis elegans*. *J Cell Biol* **180:** 357–373.

Mignolet, J., Van der Henst, C., Nicolas, C., Deghelt, M., Dotreppe, D., Letesson, J.J., and De Bolle, X. (2010) PdhS, an old-pole-localized histidine kinase, recruits the fumarase FumC in Brucella abortus. *J Bacteriol* **192:** 3235–3239.

Moreno, E., and Moriyon, I. (2006) The Genus *Brucella*. *Prokaryotes* **5:** 315–456.

Murata, T., Delprato, A., Ingmundson, A., Toomre, D.K., Lambright, D.G., and Roy, C.R. (2006) The *Legionella pneumophila* effector protein DrrA is a Rab1 guanine nucleotide-exchange factor. *Nat Cell Biol* **8:** 971–977.

Nijskens, C., Copin, R., De Bolle, X., and Letesson, J.J. (2008) Intracellular rescuing of a *B. elitensis* 16M *virB* mutant by co-infection with a wild type strain. *Microb Pathog* **45:** 134–141.

Ninio, S., and Roy, C.R. (2007) Effector proteins translocated by *Legionella pneumophila*: strength in numbers. *Trends Microbiol* **15:** 372–380.

O'Callaghan, D., Cazevieille, C., Allardet-Servent, A., Boschiroli, M.L., Bourg, G., Foulongne, V., *et al*. (1999) A homologue of the *Agrobacterium tumefaciens* VirB and *Bordetella pertussis* Ptl type IV secretion systems is essential for intracellular survival of *Brucella suis*. *Mol Microbiol* **33:** 1210–1220.

Ostrowski, M., Carmo, N.B., Krumeich, S., Fanget, I., Raposo, G., Savina, A., *et al*. (2010) Rab27a and Rab27b control different steps of the exosome secretion pathway. *Nat Cell Biol* **12:** 19–30. sup pp. 11–13.

Pizarro-Cerda, J., Meresse, S., Parton, R.G., van der Goot, G., Sola-Landa, A., Lopez-Goni, I., *et al*. (1998) *Brucella abortus* transits through the autophagic pathway and replicates in the endoplasmic reticulum of nonprofessional phagocytes. *Infect Immun* **66:** 5711–5724.

Qin, Q.M., Pei, J., Ancona, V., Shaw, B.D., Ficht, T.A., and de Figueiredo, P. (2008) RNAi screen of endoplasmic reticulum-associated host factors reveals a role for IRE1alpha in supporting *Brucella* replication. *PLoS Pathog* **4:** e1000110.

Quandt, J., and Hynes, M.F. (1993) Versatile suicide vectors which allow direct selection for gene replacement in gram-negative bacteria. *Gene* **127:** 15–21.

Raetz, C.R., and Roderick, S.L. (1995) A left-handed parallel beta helix in the structure of UDP-N-acetylglucosamine acyltransferase. *Science* **270:** 997–1000.

Raffatellu, M., Sun, Y.H., Wilson, R.P., Tran, Q.T., Chessa, D., Andrews-Polymenis, H.L., *et al*. (2005) Host restriction of *Salmonella enterica* serotype Typhi is not caused by functional alteration of SipA, SopB, or SopD. *Infect Immun* **73:** 7817–7826.

Rual, J.F., Hirozane-Kishikawa, T., Hao, T., Bertin, N., Li, S., Dricot, A., *et al*. (2004) Human ORFeome version 1.1: a platform for reverse proteomics. *Genome Res* **14:** 2128–2135.

Rual, J.F., Venkatesan, K., Hao, T., Hirozane-Kishikawa, T., Dricot, A., Li, N., *et al*. (2005) Towards a proteome-scale map of the human protein-protein interaction network. *Nature* **437:** 1173–1178.

Sambrook, J., and Russel, D.W. (2001) *Molecular Cloning, A Laboratory Manual Cold Spring Harbour*. New York: Cold Spring Harbour Laboratory Press, pp. 2,344.

Seabra, M.C., Mules, E.H., and Hume, A.N. (2002) Rab GTPases, intracellular traffic and disease. *Trends Mol Med* **8:** 23–30.

Sherman, F. (1991) Getting started with yeast. *Methods Enzymol* **194:** 3–21.

Shohdy, N., Efe, J.A., Emr, S.D., and Shuman, H.A. (2005) Pathogen effector protein screening in yeast identifies *Legionella* factors that interfere with membrane trafficking. *Proc Natl Acad Sci USA* **102:** 4866–4871.

Simon, R., Priefer, U., and Pühler, A. (1983) A broad host range mobilization system for *in vivo* genetic engineering: transposon mutagenesis in Gram negative bacteria. *Nat Biotechnol* **1:** 784–791.

Smith, A.C., Heo, W.D., Braun, V., Jiang, X., Macrae, C., Casanova, J.E., *et al*. (2007) A network of Rab GTPases controls phagosome maturation and is modulated by *Salmonella enterica* serovar Typhimurium. *J Cell Biol* **176:** 263–268.

Stuart, L.M., Boulais, J., Charriere, G.M., Hennessy, E.J., Brunet, S., Jutras, I., *et al*. (2007) A systems biology analysis of the Drosophila phagosome. *Nature* **445:** 95–101.

Takai, Y., Sasaki, T., and Matozaki, T. (2001) Small GTP-binding proteins. *Physiol Rev* **81:** 153–208.

Thery, C., Duban, L., Segura, E., Veron, P., Lantz, O., and Amigorena, S. (2002) Indirect activation of naive CD4+ T cells by dendritic cell-derived exosomes. *Nat Immunol* **3:** 1156–1162.

Tisdale, E.J., Bourne, J.R., Khosravi-Far, R., Der, C.J., and Balch, W.E. (1992) GTP-binding mutants of rab1 and rab2 are potent inhibitors of vesicular transport from the endoplasmic reticulum to the Golgi complex. *J Cell Biol* **119:** 749–761.

Tisdale, E.J., Azizi, F., and Artalejo, C.R. (2009) Rab2 utilizes glyceraldehyde-3-phosphate dehydrogenase and protein kinase C(iota) to associate with microtubules and to recruit dynein. *J Biol Chem* **284:** 5876–5884.

Vergunst, A.C., van Lier, M.C., den Dulk-Ras, A., Stuve, T.A., Ouwehand, A., and Hooykaas, P.J. (2005) Positive charge is an important feature of the C-terminal transport signal of the VirB/D4-translocated proteins of *Agrobacterium*. *Proc Natl Acad Sci USA* **102:** 832–837.

Vidal, M., Brachmann, R.K., Fattaey, A., Harlow, E., and Boeke, J.D. (1996) Reverse two-hybrid and one-hybrid systems to detect dissociation of protein-protein and DNA-protein interactions. *Proc Natl Acad Sci USA* **93:** 10315–10320.

Vidalain, P.O., Boxem, M., Ge, H., Li, S., and Vidal, M. (2004) Increasing specificity in high-throughput yeast two-hybrid experiments. *Methods* **32:** 363–370.

Walhout, A.J., and Vidal, M. (2001) High-throughput yeast two-hybrid assays for large-scale protein interaction mapping. *Methods* **24:** 297–306.

Walhout, A.J., Temple, G.F., Brasch, M.A., Hartley, J.L., Lorson, M.A., van den Heuvel, S., and Vidal, M. (2000) Gateway recombinational cloning: application to the cloning of large numbers of open reading frames or ORFeomes. *Methods Enzymol* **328:** 575–592.

Wang, Y., Cui, T., Zhang, C., Yang, M., Huang, Y., Li, W., *et al*. (2010) Global protein-protein interaction network in the human pathogen *Mycobacterium tuberculosis* H37Rv. *J Proteome Res* **9:** 6665–6677.

Young, G.M., Schmiel, D.H., and Miller, V.L. (1999) A new pathway for the secretion of virulence factors by bacteria: the flagellar export apparatus functions as a protein-secretion system. *Proc Natl Acad Sci USA* **96:** 6456–6461.

Supporting information

Additional Supporting Information may be found in the online version of this article:

Table S1. DB-X plates organization.
Table S2. 144 human–Brucella interaction pairs produced by the HT-Y2H screen.
Table S3. 21 interactions confirmed between human and *B. melitensis* proteins using Y2H.
Table S4. List of the 103 predicted human proteins homologous to small GTPases.

Please note: Wiley-Blackwell are not responsible for the content or functionality of any supporting materials supplied by the authors. Any queries (other than missing material) should be directed to the corresponding author for the article.